

Article

Fatigue Strength Assessment of an Aluminium Alloy Car Body Using Multiaxial Criteria and Cumulative Fatigue Damage Theory

Yiming Shangguan ^{1,2}, Wenjing Wang ^{2,*}, Chao Yang ² and Anrui He ¹

¹ National Engineering Technology Research Center of Flat Rolling Equipment, University of Science and Technology Beijing, Beijing 100083, China

² School of Mechanical, Electronic and Control Engineering, Beijing Jiaotong University, Beijing 100044, China

* Correspondence: wjwang@bjtu.edu.cn

Abstract: With the rapid development of urban rail transit, metro vehicles have become preferred choices for urban transportation. It is important to accurately evaluate the fatigue strength of a car body to ensure subway safety. A new method based on multiaxial stress criteria and cumulative fatigue damage theory was proposed for the fatigue strength assessment of welded joints of an aluminium alloy head car body subjected to variable cyclic loads. A local coordinate system was established, according to the geometrical characteristics of the weld. Local stresses perpendicular and parallel to the weld seam were obtained to calculate the stress ratio, stress range, and allowable stress value corresponding to the stress component. Then, the fatigue strength utilization of the joints was estimated to determine whether the fatigue strength of the weld met the design requirements. Moreover, the estimated fatigue life of the car body was predicted with cumulative fatigue damage theory. This method considers both the material utilization degree in multiple stress states and the estimated body fatigue life of the car body. The research results provide a reference and a more comprehensive guarantee for the fatigue strength evaluation of a subway car body's welded structure to ensure vehicle safety.



Citation: Shangguan, Y.; Wang, W.; Yang, C.; He, A. Fatigue Strength Assessment of an Aluminium Alloy Car Body Using Multiaxial Criteria and Cumulative Fatigue Damage Theory. *Appl. Sci.* **2023**, *13*, 215. <https://doi.org/10.3390/app13010215>

Academic Editors: Alberto Campagnolo and Alberto Sapora

Received: 28 November 2022

Revised: 18 December 2022

Accepted: 21 December 2022

Published: 24 December 2022



Copyright: © 2022 by the authors. Licensee MDPI, Basel, Switzerland. This article is an open access article distributed under the terms and conditions of the Creative Commons Attribution (CC BY) license (<https://creativecommons.org/licenses/by/4.0/>).

Keywords: fatigue strength assessment; aluminium alloy car body; multiaxial criteria; cumulative fatigue damage theory; welded joints

1. Introduction

Fatigue has been researched for decades as one of the most common failure modes of mechanical structures. The fatigue damage assessment approaches of welded structures include the hot spot stress method, effective notch stress method, etc. The hot spot stress is related to the overall geometry and load conditions of the welded structure, but does not include the stress concentration caused by local factors, such as weld size and welding defects [1,2]. W J Wang et al. [3] used the hot spot stress method to calculate the hot spot stress value at the welding toe, and a modified S–N curve, considering the thickness effect of the main board, was proposed to predict the fatigue life of the sample. B J Wang et al. [4] compared the hot spot stress calculation result with the nominal stress from shell elements in a welded bogie frame, and their results showed that the hot spot stress is higher than the nominal stress. Z Y Zhou et al. [5] clarified the limitations of the hot spot stress method. These researchers proposed that the hot spot stress method could effectively evaluate toe failure based on the geometric discontinuity of the welding structure, but could not appraise the fatigue failure caused by defects on the weld root and inside the weld. This method is suitable for the fatigue analysis of the toe of nonstandard structural details and complex welding joints. The effective notch stress method uses a specific radius to replace the notch at the weld root and toe and calculates the effective notch stress at the weld toe and weld root by the finite element method (FEM). This approach avoids the occurrence of

singular stress values at the sharp gap and can be used for fatigue evaluation at the weld root and toe [6,7]. It can also determine whether fatigue failure occurs at the weld root or toe by assessing principal stress. W Shen et al. [8] estimated the fatigue life of welded joints, and their results indicated that this method can rationalize the thickness effect observed in these joints. Xu Liu et al. [9,10] obtained the stress concentration coefficient of a welded joint gap by using a formula method and numerical method. These researchers obtained an S–N curve with a lower slope than the FAT225 curve recommended by the International Welding Society (IIW). At present, if the effective notch stress method or hot spot stress method is adopted for the analysis of a car body, then the required grid division of the weld area is exceedingly small, leading to an excessively large number of grids at the weld area. Furthermore, an abrupt change in the grid size in the transition area between large and small grids may occur, which is inappropriate in engineering. This method is not sensitive to the grid and has a high calculation accuracy. The effects of stress concentration, plate thickness, and load mode on fatigue life can be considered simultaneously [11]. S M Xie [12] used the structural stress method to predict the fatigue life of the welded structure of rail vehicles. The calculation steps were complicated, and the resulting data could not be directly mapped to each node in the weld model. The nominal stress method has been broadly used in fatigue assessment [13–16]. This method references a defined component cross-section and neglects the local peak stresses resulting from geometrical notches or load applications. The fatigue strength of a structure can be directly estimated according to the nominal structural stress and the S–N curve corresponding to different notch grades. This method has three advantages when using the FEM to solve engineering problems: the methodology is straightforward; the mesh quality requirement is low; the nominal stress value is accessible. However, the dispersion between the fatigue life and nominal stress amplitude is large, and it is difficult to obtain accurate prediction results. The multiaxial stress method [17,18] is more comprehensive and accurate than the uniaxial stress method. Specifically, the fatigue evaluation method comprehensively considers the spatial stress states of the evaluation points. Current research papers on transforming multiaxial stress into uniaxial stress are as follows. P P Zhang et al. [19] projected multiaxial stress and evaluated the fatigue strength of electric multiple unit (EMU) wheels based on the principal stress method. A Qi et al. [20] established a weld coordinate system according to geometric features and calculated the stress components of nodes under a multiaxial stress state to perform a fatigue life analysis method for a freight car body. These investigators concluded that using the multiaxial stress method to evaluate fatigue strength is beneficial for the lightweight design of a car body. In the above studies, the appropriate evaluation methods were selected mainly according to the specific engineering requirements. While many factors can affect welded joint fatigue, the majority of the current research has only focused on one aspect. Further studies are needed to address the common impacts of multiple factors.

The car body is the main bearing structure of a subway vehicle, which is located on a bogie and bears various dynamic and static loads during operation. Fatigue failure is one of the most critical failure modes of car body structures; hence, its fatigue strength analyses are of vital importance to ensure reliable performance. Compared with a carbon steel car body, an aluminium alloy car body offers the following advantages: lightweight body structure, high corrosion resistance, excellent extrusion resistance, and low overall cost. For aluminium alloy materials, the fatigue strength of a welded joint is approximately half that of the base metal, so compared with the welded joint, the base metal is not prone to fatigue failure. As a consequence, the fatigue strength evaluation of an aluminium alloy car body typically focuses on the welded joints [21].

This paper proposes a method that combines the nominal stress method and multiaxial stress method based on multiaxial stress criteria and the fatigue cumulative fatigue damage theory, according to the DVS 1608 standard [22] and EN 1999 standard [23], respectively. This method is accurate and efficient, since it not only considers the material utilization degree in multiple structural directions to demonstrate the comprehensive degree of utiliza-

tion of the pivotal weld joints, but also shows the estimated fatigue life of the aluminium alloy car body.

2. Theoretical Background

2.1. Multiaxial Stress Criteria

The head car body is affected not only by the aerodynamic load, but also by the brake friction, vibration, and other alternating mechanical loads during operation. Thus, the head car body's stress distribution is a multiaxial stress state, which cannot be directly used for fatigue life assessment. Therefore, the stress component in a global coordinate system needs to be converted into a local coordinate system to obtain relevant fatigue parameters. That is, the stress components need to be evaluated at the weld position, which includes the axial force parallel to and perpendicular to the weld direction (σ_{\parallel} and σ_{\perp}) and the shear stress (τ_{\parallel}), as shown in Figure 1:

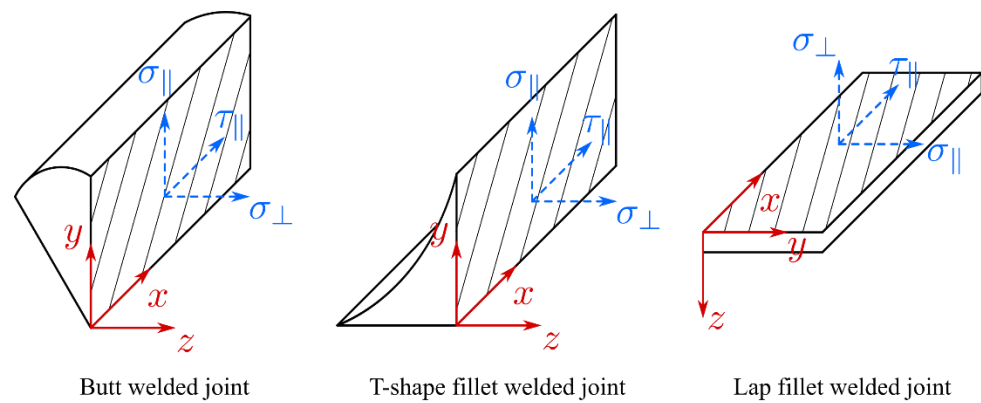


Figure 1. Stress components decomposition of welded joints in the local coordinate system.

The stress components of the node in the global coordinate system include normal stress components ($\sigma_x, \sigma_y, \sigma_z$) and shear stress components ($\tau_{xy}, \tau_{yz}, \tau_{xz}$). The transformation formula for the node stress components to a different coordinate system is as follows:

$$\sigma_{j'k'} = \alpha_{j'j} \alpha_{k'k} \sigma_{jk} \tag{1}$$

$$\sigma_{j'} = \alpha_{j'1}^2 \sigma_1 + \alpha_{j'2}^2 \sigma_2 + \alpha_{j'3}^2 \sigma_3 \tag{2}$$

where $\sigma_{j'k'}$ is the second-order stress tensor in the local coordinate system, $\alpha_{j'j}$ and $\alpha_{k'k}$ are the direction cosine between the corresponding directions of the two coordinate systems. $\sigma_{j'}$ is the principal stress in the local coordinate system.

After the transformation, the normal stress and corresponding shear stress in the local coordinate system at the critical position of the weld were extracted. Then, the utilization degree ($a_{\perp}, a_{\parallel}, a_{\tau}$) in the local coordinate system were evaluated according to Equations (3)–(5). Fatigue calculations should be conducted for each stress component:

$$a_{\perp} = \left| \frac{\sigma_{\perp}}{[\sigma_{\perp}]} \right| \leq 1 \tag{3}$$

$$a_{\parallel} = \left| \frac{\sigma_{\parallel}}{[\sigma_{\parallel}]} \right| \leq 1 \tag{4}$$

$$a_{\tau} = \left| \frac{\tau_{\parallel}}{[\tau_{\parallel}]} \right| \leq 1 \tag{5}$$

In addition, the influence of multiaxial stress satisfies Equation (6):

$$\alpha_v = \sqrt{(a_{\perp})^2 + (a_{\parallel})^2 + f_v \cdot (a_{\perp}) \cdot (a_{\parallel}) + (a_{\tau})^2} \leq 1 \tag{6}$$

The fatigue strength of the welding site is independent of the base metal alloy and only depends on the stress ratios R_σ and R_τ . The stress ratio is equal to the minimum stress divided by the maximum stress. The notch condition curve index x is given in the appendix of DVS1608. In addition, the values of medium stress sensitivity for the medium stress effect and internal stress effect are used for welding joints of aluminium alloys in railway vehicle manufacturing. The allowable fatigue stress amplitude of axial stress σ_\perp and σ_\parallel are obtained through Equations (7)–(10) [22].

Interval 1: $R_\sigma > 1$

$$[\sigma_{(R)}] = 54 \cdot 1.04^{-x} \tag{7}$$

Interval 2: $R_\sigma \leq 0$

$$[\sigma_{(R)}] = 46 \cdot 1.04^{-x} \left(\frac{1}{1 + M_\sigma \frac{1+R_\sigma}{1-R_\sigma}} \right) \tag{8}$$

Interval 3: $0 < R_\sigma < 0.5$

$$[\sigma_{(R)}] = 42 \cdot 1.04^{-x} \left(\frac{1}{1 + \frac{M_\sigma}{3} \frac{1+R_\sigma}{1-R_\sigma}} \right) \tag{9}$$

Interval 4: $0.5 \leq R_\sigma < 1$

$$[\sigma_{(R)}] = 36.5 \cdot 1.04^{-x} \tag{10}$$

Note that there is no case for $R_\sigma = 1$, since it refers to a quasi-static stress state (the maximum stress equals the minimum stress).

The allowable fatigue stress amplitude of shear stress τ_\parallel is obtained from Equations (11)–(13). For shear stress, there is no interval 1, and interval 2 has a minimum value of variation, which is contrary to the axial stress calculated in Equations (7)–(10) [22].

Interval 2: $-1 \leq R_\tau \leq 0$

$$[\tau_{(R)}] = 28 \cdot 1.04^{-x} \left(\frac{1}{1 + M_\tau \frac{1+R_\tau}{1-R_\tau}} \right) \tag{11}$$

Interval 3: $0 < R_\tau < 0.5$

$$[\tau_{(R)}] = 26.5 \cdot 1.04^{-x} \left(\frac{1}{1 + \frac{M_\tau}{3} \frac{1+R_\tau}{1-R_\tau}} \right) \tag{12}$$

Interval 4: $R_\tau \geq 0.5$

$$[\tau_{(R)}] = 24.4 \cdot 1.04^{-x} \tag{13}$$

2.2. Cumulative Fatigue Damage Theory

Cumulative fatigue damage is a material mechanical property deterioration process caused by repeated cyclic stress. Fatigue failure occurs when damage accumulates to a critical value. The accurate description of the material fatigue cumulative damage development process under cyclic loading is the basis of material fatigue life estimations and rational structure fatigue design. The default S–N curve data are measured under the same stress amplitude when using the S–N curve for fatigue life evaluation, as shown in Figure 2. The stress applied to a structure is complex and changeable in practical engineering problems, so the fatigue life cannot be obtained directly using the S–N curve. Miner’s linear damage accumulation theory solves this problem well and plays a role as a bridge. Miner’s linear fatigue cumulative damage theory considers fatigue failure an

irreversible deterioration process of materials under cyclic stress. Each internal change in the structure itself is related to the external loading mode in this state.

$$\frac{n}{N} = \begin{cases} 2 \times 10^6 \left(\frac{\Delta\sigma_c}{\Delta\sigma_i} \times \frac{1}{\gamma_{Ff} \times \gamma_{mf}} \right)^{m_1} & (10^5 \leq N \leq 5 \times 10^6) \\ 5 \times 10^6 \left(\frac{\Delta\sigma_c}{\Delta\sigma_i} \times \frac{1}{\gamma_{Ff} \times \gamma_{mf}} \right)^{m_2} \left(\frac{2}{5} \right)^{\frac{m_2}{m_1}} & (5 \times 10^6 \leq N \leq 10^8) \end{cases} \quad (14)$$

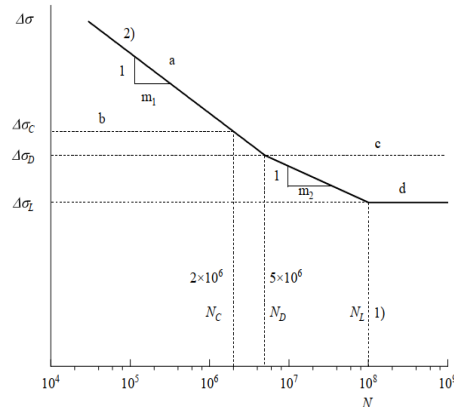


Figure 2. A typical fatigue strength S-N curve [23]; a—fatigue strength curve; b—reference fatigue strength; c—constant amplitude fatigue limit; and d—cut-off limit; m_1 and m_2 are the slope of the curve, $m_2 = m_1 + 2$.

The life prediction algorithm in the EN1999 standard is based on Palmgren–Miner cumulative damage theory, which calculates the damage generated by each load case under fatigue load conditions and accumulates the damage generated by all load cases to obtain the total damage. The calculation formula is shown in Equations (15) and (16):

$$\frac{n_i}{N_i} = \left(\frac{\sigma}{\sigma_{-1}} \right)^m \quad (15)$$

$$D = \sum \left(\frac{n_i}{N_i} \right) = \frac{n_1}{N_1} + \frac{n_2}{N_2} + \dots + \frac{n_n}{N_n} \quad (16)$$

3. Numerical Simulations

3.1. Main Structure

A head car body is a lightweight, monocoque cylindrical structure welded from large-section aluminium profiles and plates. This structure is designed mainly to carry all the equipment and personnel of the vehicle and provide installation interfaces for vehicle equipment. The roof, sidewalls, end walls, and underframe of the aluminium head car body contain welded structures. Figure 3 presents three typical welding forms, including butt-welded joints, T-shaped fillet-welded joints, and lap fillet-welded joints, which are located in the sidewalls, the driver’s cab, and the underframes, respectively. When evaluating the fatigue strength in the ANSYS platform, the stress in the overall Cartesian coordinate system should be converted to a local coordinate system, since the program cannot directly identify the evaluating nodes. Therefore, the sets of welded locations corresponding to the local coordinate system should be established one-to-one during modelling. The program evaluates the nodes in the set, according to the direction of the local coordinate system. The assessed position of each weld is marked with white points in the finite element diagram, and two rows of nodes with a distance of 5 mm from the weld are taken as evaluation points (see the insertion at the right end of Figure 3). In addition, the length of the strain gauge is ignored, so the calculated results are conservative.

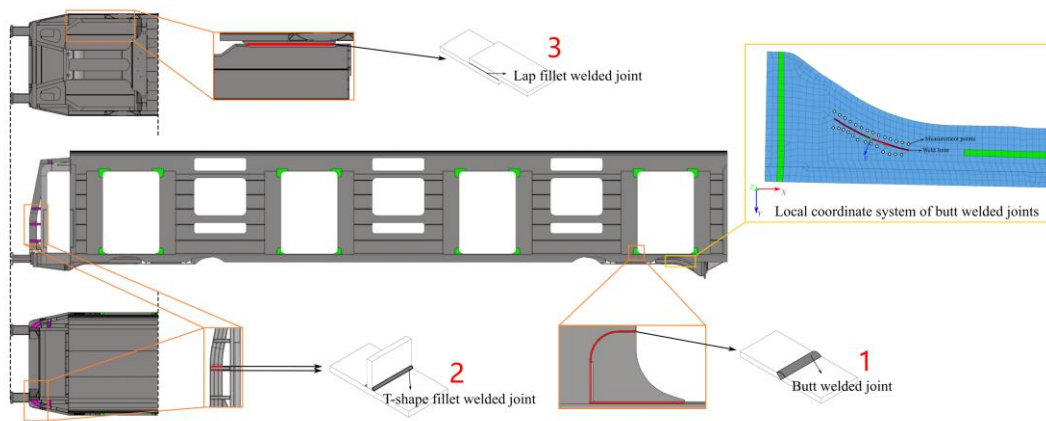


Figure 3. Schematic diagram of the head car body.

3.2. Standard Prescribed Loads

EN12663 [24] stipulates that the rail vehicle body structure bears multiple dynamic loads, to different extents, during its operating life. Research on car body fatigue life should consider the effects of cyclic loads as they lead to fatigue failure. This fatigue assessment specifies ± 0.15 g as the acceleration amplitude. Individual stress values have a negligible influence on fatigue life, but stress amplitude can dramatically affect fatigue performance. In practice, the actual operation loads for the vehicles are complicated, and to simplify the problem, we defined four basic load scenarios, regarding load directions and types: longitudinal loads (in the X-direction), lateral loads (in the Y-direction), vertical loads (in the Z-direction), and additional load (line twisting load). To reproduce the actual load conditions, the four basic load cases are arranged in a rational way and extended to 28 different load cases, as shown in Table 1. An ANSYS subroutine was established to handle these load cases and output the stress information needed for further analysis, including the maximum, minimum stress in each direction, and stress amplitudes for each type of welded joint.

Table 1. Cyclic load cases for fatigue strength assessment.

Load Case	Acceleration (m/s ²)			Additional Load	Load Case	Acceleration (m/s ²)			Additional Load
	X	Y	Z			X	Y	Z	
1	+0.15 g		1 g		15	+0.15 g		1 g	
2	-0.15 g		1 g		16	-0.15 g		1 g	
3		+0.15 g	1 g		17		+0.15 g	1 g	
4		-0.15 g	1 g		18		-0.15 g	1 g	
5			0.85 g		19			0.85 g	
6			1.15 g		20			1.15 g	
7	+0.15 g	+0.15 g	0.85 g	/	21	+0.15 g	+0.15 g	0.85 g	21 mm
8	+0.15 g	-0.15 g	0.85 g		22	+0.15 g	-0.15 g	0.85 g	
9	-0.15 g	+0.15 g	0.85 g		23	-0.15 g	+0.15 g	0.85 g	
10	-0.15 g	-0.15 g	0.85 g		24	-0.15 g	-0.15 g	0.85 g	
11	+0.15 g	+0.15 g	1.15 g		25	+0.15 g	+0.15 g	1.15 g	
12	+0.15 g	-0.15 g	1.15 g		26	+0.15 g	-0.15 g	1.15 g	
13	-0.15 g	+0.15 g	1.15 g		27	-0.15 g	+0.15 g	1.15 g	
14	-0.15 g	-0.15 g	1.15 g		28	-0.15 g	-0.15 g	1.15 g	

3.3. Fatigue Assessment Process

Figure 4 illustrates the fatigue assessment flow based on multiaxial stress criteria and cumulative fatigue damage theory. The assessment process was programmed by using the APDL language in ANSYS. The design loads prescribed by standards were used to assess the structure’s fatigue. These cyclic loads were first applied to the head car body models. Then, numerical calculations were carried out by the FEM to obtain stress distributions. According to the multiaxial stress criteria, the normal stress and shear stress in the local

coordinate system were extracted. In addition, the notch curve index x was selected according to the welded joint shape, and then the allowable normal stresses along and perpendicular to the weld direction, as well as the allowable shear stress, were calculated. After that, the fatigue strength utilization of the joints was estimated to determine whether the fatigue strength of the weld met the design requirements. In addition, when the maximum allowable stress and the stress ratio were both inside the Moore–Kommers–Jasper (MKJ) diagram, the head car body fatigue life could satisfy the design requirements. According to cumulative fatigue damage theory, the damage generated by all load cases was accumulated to obtain the total damage and the estimated fatigue life.

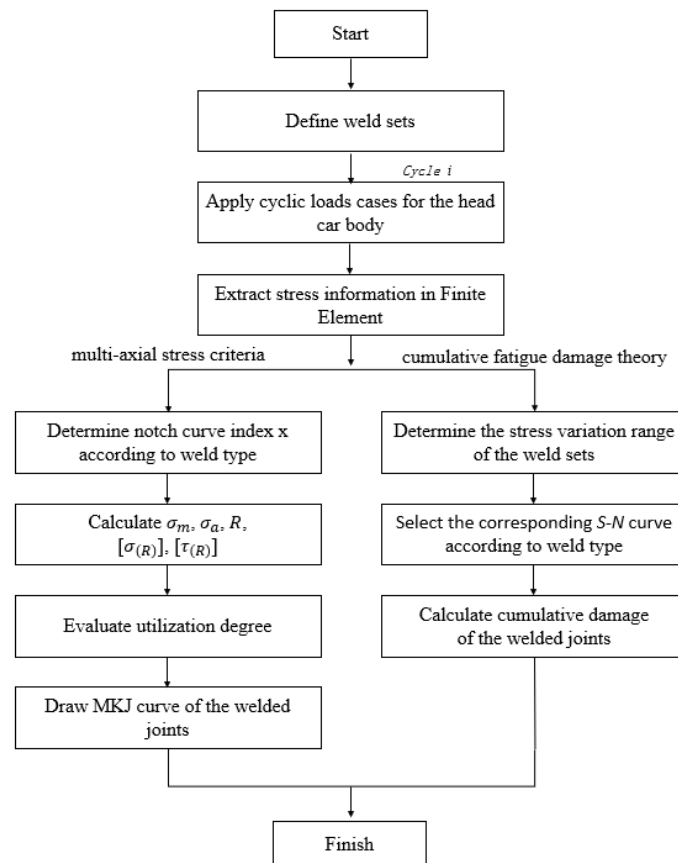


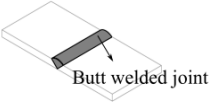
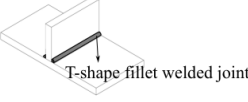
Figure 4. Flow chart of the fatigue life evaluation based on two methods.

3.4. Fatigue Strength Value Selection

Table 2 presents the notch curve, and its index x (specified in DVS 1608 [22]) selected for different weld types for usage in the multi-axis stress method, the structural classification (detail type and category, specified in EN1999 [23]), and the allowable stress range $\Delta\sigma$ (at $N = 1 \times 10^7$) for usage in the cumulative damage method. Figures 5 and 6 illustrate the S-N curves for different weld types. For multi-axis stress method, after all the 28 load cases in Table 1 were input into the ANSYS subroutine and the corresponding local stress states were calculated, the maximum and minimum local stresses (among all 28 load cases) in each direction (σ_{\perp} , σ_{\parallel} , τ_{\parallel}), for each type of welded joint, were extracted (see Table 3). As for the cumulative damage method, each type of the welded joint was given an S-N curve (either from Figure 5 or Figure 6), referring to standard EN1999. For example, a butt-welded joint with detail type number 7.3.1 in EN1999 was found to have an identical configuration as the butt weld we studied, and its detail category was illustrated as 40-4.3 (40 refers to the stress range at $N = 2 \times 10^6$, and 4.3 refers to the line slope of m_1 , as sketched in Figure 2. Others follow the same naming rule); hence, the S-N curves in Figure 5, with 40-4.3 marked at the right end side, were selected. N is then evaluated based on the calculated stress range S with the aforeslected curve. Here, except for N , we also introduced the allowable

stress range $\Delta\sigma$, which was defined at $N = 1 \times 10^7$, to serve as an additional reference that could make the data process procedure simpler and more intuitive. Note that, for stress ranges that were lower than the cut-off limit, which corresponds to $N \geq 10^8$, the damage was zero.

Table 2. Detailed categories for three welded joints between members.

Constructional Detail Initiation Site	Curve (σ_{\parallel})	x (σ_{\parallel})	Curve (σ_{\perp})	x (σ_{\perp})	Curve (τ)	x (τ)	Detail Type	Detail Category	$\Delta\sigma _{N=1 \times 10^7}$ (MPa)
 Butt welded joint	D	12	E1	15	G	0	7.3.1	40-4.3	29.0
 T-shape fillet welded joint	C-	10	E5	21	H	9	9.2	25-3.4	16.8
 Lap fillet welded joint	F2	41	D	12	H	9	9.4	23-3.4	15.5

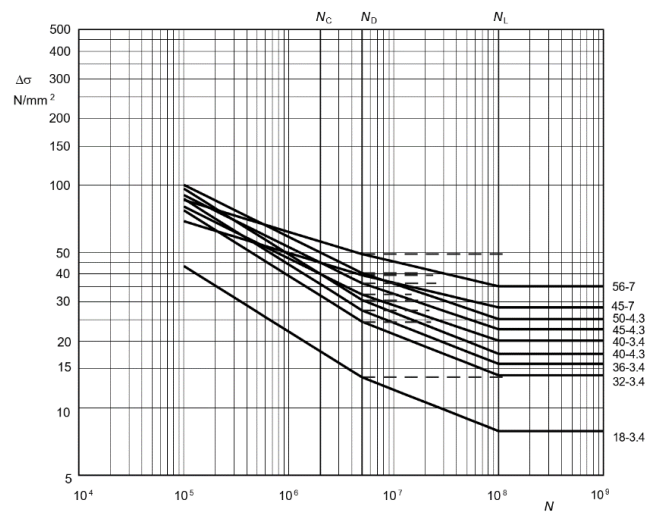


Figure 5. S-N curves for butt-welded joint [23].

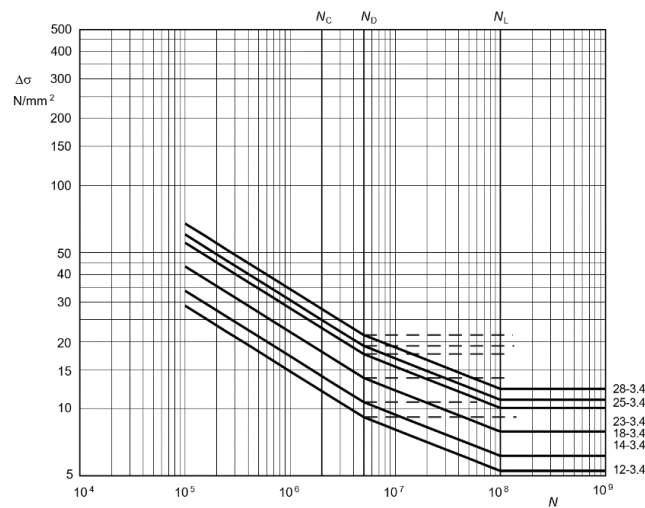


Figure 6. S-N curves for T-shaped welded joint and lap fillet-welded joint [23].

Table 3. Fatigue evaluation assessment results.

Weld Position	σ_m	σ_a	σ_{min}	σ_{max}	R	$1/R$	M_σ	$[a_\perp]$	σ_{min} Case	σ_{max} Case	
1	19.01	3.29	15.72	22.31	0.70	1.42	0.30	22.80	7	28	
2	5.50	1.26	4.24	6.76	0.63	1.59	0.30	24.66	24	11	
3	10.02	2.29	7.73	12.31	0.63	1.59	0.30	7.31	8	27	
Weld Position	σ_m	σ_a	σ_{min}	σ_{max}	R	$1/R$	M_σ	$[a_\parallel]$	σ_{min} Case	σ_{max} Case	
1	-22.49	3.90	-26.39	-18.59	1.42	0.70	0.30	29.98	27	8	
2	-8.15	2.22	-10.37	-5.93	1.75	0.57	0.30	23.70	11	24	
3	-9.98	2.23	-12.21	-7.76	1.57	0.64	0.30	33.73	25	10	
Weld Position	τ_m	τ_a	τ_{min}	τ_{max}	R	$1/R$	M_τ	$[a_\tau]$	τ_{min} Case	τ_{max} Case	
1	5.84	1.03	4.82	6.87	0.70	1.43	0.17	24.40	8	27	
2	2.88	0.72	2.15	3.60	0.60	1.67	0.17	17.14	9	26	
3	7.55	1.63	5.93	9.18	0.65	1.55	0.17	17.14	7	28	
Weld Position	Normal Stress σ_\perp			Normal Stress σ_\parallel			Shear Stress τ_\parallel			α_v	Assessment
	σ_a	$\sigma_{a,zul}$	a_\perp	σ_a	$\sigma_{a,zul}$	a_\parallel	τ_a	$\tau_{a,zul}$	a_τ		
1	3.29	22.80	0.14	3.90	29.98	0.13	1.03	24.40	0.04	0.20	Pass
2	1.26	24.66	0.05	2.22	23.70	0.09	0.72	17.14	0.04	0.10	Pass
3	2.29	7.31	0.31	0.25	33.73	0.01	1.63	17.14	0.10	0.33	Pass

4. Results and Discussion

4.1. Stress Component Calculation

Table 3 lists the evaluation results of the three weld positions, where positions 1, 2, and 3 refer to the butt-welded joint, T-shape welded joint, and lap fillet-welded joint, respectively (see Figure 3). The subscripts m , a , min , max of σ and τ refer to the mean, amplitude, minimum, and maximum of the stress, respectively. The minimum and maximum normal and shear stress were extracted by subroutine, and the corresponding minimum and maximum load cases are listed in Table 3. The results indicate that the main factors affecting the butt-welded joints are the normal stresses perpendicular and parallel to the direction of the weld ($a_\perp = 0.14$, $a_\parallel = 0.13$). The main factor affecting the T-shaped fillet-welded joints was the normal stress perpendicular to the direction of the weld ($a_\parallel = 0.09$). The main factor affecting the lap fillet-welded joints was the normal stress perpendicular to the direction of the weld, with the largest utilization degree under normal stress in the x-direction of local coordinates ($a_\perp = 0.31$). The normal stress parallel to the lap fillet weld had negligible influence. In addition, the lap-welded joints exhibited the highest comprehensive degree of utilization of 0.33, and the T-shaped fillet-welded joints demonstrated the lowest comprehensive degree of utilization of 0.10. The results show that the components and comprehensive degree of the utilization of the pivotal weld joints in the aluminium alloy car body were less than 1, and the normal stress and shear stress of the welded seam of the car body structure were both within the MKJ fatigue evaluation curve, which also indicates that the fatigue failure of welded joints of the head car body first occurred in the lap-welded joint.

In the MKJ diagram, the horizontal axis is the stress ratio R , the vertical axis is the maximum allowable stress corresponding to the stress ratio, the numbers above the curve refer to the corresponding allowable stress, and the nodes below the curve refer to the calculation results of the measurement points on the welded positions. If the calculation results fell under the fatigue strength curves, then the fatigue performance of the welded structure met the standard requirements. The maximum and minimum normal stresses were obtained by plane stress calculation, and the allowable stresses of the corresponding components were obtained by the evaluation process. After data processing, the calculated

results of the directional stress of all three welds in the car body were drawn in the MKJ curve of the corresponding welded joint. Figures 7–9 illustrates the three typical weld joints.

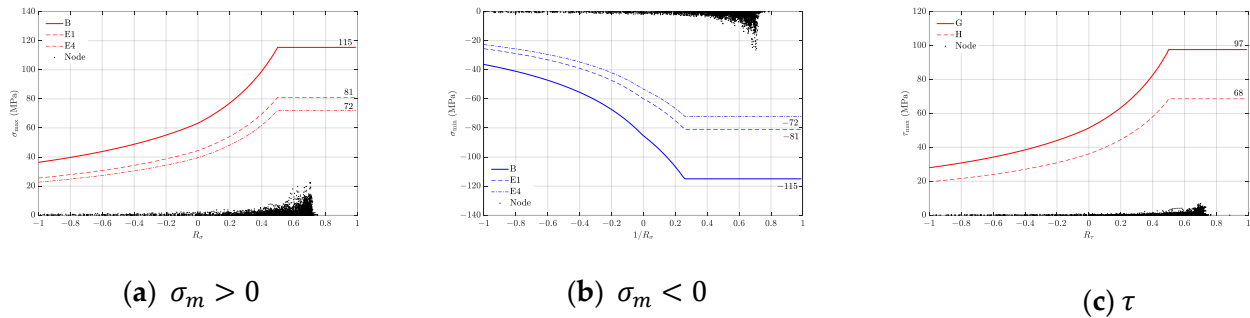


Figure 7. MKJ fatigue characteristic curve at weld position 1 in the sidewall.

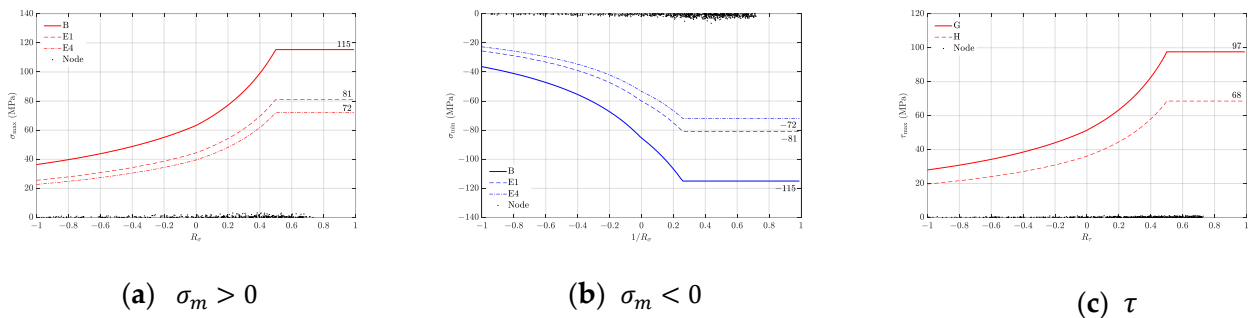


Figure 8. MKJ fatigue characteristic curve at weld position 2 in the driver's cab.

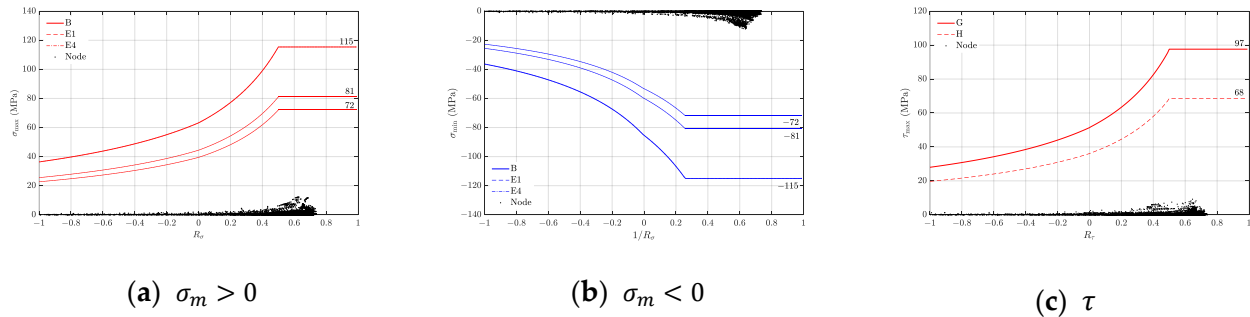


Figure 9. MKJ fatigue characteristic curve at weld position 3 in the underframe area.

4.2. Fatigue Life Prediction

The allowable fatigue stress at load cycles of 1×10^7 on the corresponding stress range curve was obtained for the three weld positions. Table 4 lists the calculation results and the top ten algebraic values under different load cases. The node number refers to the evaluation node set's identifiers of three weld positions in finite element software. According to the results of the fatigue life calculation, the most critical areas were the lap fillet-welded joint (node 2,060,984), with a fatigue life of 1.64×10^7 , followed by butt-welded joints, with a fatigue life of 1.82×10^7 . The T-shaped fillet-welded joints generated the greatest fatigue life of 2.14×10^7 . The results indicate that, under all fatigue conditions, the calculated life of the welded positions met the requirement of minimum load cycles of 1×10^7 and showed no hidden danger of fatigue failure.

Table 4. Fatigue evaluation assessment results at various weld positions (MPa).

Weld Position 1			Weld Position 2			Weld Position 3		
Node Number	Fatigue Life (10^7)	Fatigue Damage (10^{-8})	Node Number	Fatigue Life (10^7)	Fatigue Damage (10^{-8})	Node Number	Fatigue Life (10^7)	Fatigue Damage (10^{-8})
1,564,148	1.82	5.49	1,782,584	2.14	4.67	2,060,984	1.64	6.10
1,564,147	1.82	5.49	16	2.24	4.46	1,983,385	1.72	5.81
1,564,144	2.45	4.08	1,836,330	2.50	4.00	2,000,234	1.75	5.71
1,564,145	3.04	3.29	1,836,332	2.59	3.86	2,060,972	1.79	5.59
2,073,400	3.80	2.63	60,638	2.60	3.85	1,585,000	1.90	5.26
1,899,942	5.21	1.92	60,640	2.67	3.75	2,067,444	1.91	5.24
1,562,037	5.25	1.90	1,836,333	2.65	3.77	1,989,300	2.01	4.98
1,899,921	5.26	1.90	1,782,579	2.69	3.72	2,041,772	1.91	5.24
1,562,030	5.35	1.87	60,641	2.73	3.66	1,566,194	1.92	5.21
1,899,949	5.40	1.85	1,782,576	2.80	3.57	1,587,979	2.22	4.50

5. Conclusions

This paper proposes a new method for combining multiaxial stress criteria and cumulative fatigue damage theory to evaluate the fatigue strength of three typical welded joints (butt-welded joints, T-shaped fillet-welded joints, and lap fillet-welded joints) in an aluminium alloy head car body. The results indicate that, for the aforementioned car body configuration and load cases, the T-shaped fillet-welded joint exhibited excellent fatigue failure resistance, as it holds the lowest utilization degree and the highest fatigue life expectation. In contrast, the lap-welded joint showed the worst capability to resist fatigue failure, as it has the highest utilization degree and the lowest fatigue life. Regardless, all the welded joints tested in this paper complied with the fatigue safety requirements.

This method is accurate and efficient, since it not only considers the material utilization degree in multiple stress states, but also accounts for the estimated fatigue life of the car body. Designers can determine the safety margin of a structure by comparison with a utilization degree of 1. In addition, the weak area of weld fatigue can be accurately predicted, and the structure's fatigue life can be determined. This method provides certain guidance and a theoretical basis for the fatigue evaluation of subway car body welded structures. The fatigue strength of welded structures can be improved in the following ways:

- The welding type can be changed, and the notch line grade can be improved to increase the allowable fatigue stress. For instance, lap fillet-welded joints can be changed to butt-welded joints, partial penetration can be changed to full penetration, and single-sided welding can be changed to double-sided welding. By doing so, a smaller value of index x can be achieved, which corresponds to higher allowable fatigue stress (Equations (7)–(13)) and a lower utilization degree (Equations (3)–(5)), both of which contribute to a safer weld bounding.
- The structure can be optimized to reduce the stress range of the welded joints. The notch line grade can be improved through weld processing techniques, such as weld grinding.
- In the design stage, the reinforcement can be arranged in the appropriate position of the fatigue assessment danger point to reduce the peak stress of the dangerous area and reduce the utilization of the weld material.
- In the construction process, the level of post-welding treatment in dangerous areas should be improved, and more detailed flaw detection should be carried out.
- In daily operation and maintenance, we should also focus on whether fatigue cracks occur in this area to ensure driving safety.

Author Contributions: The author's contributions are as follows: W.W. performed the conceptualization, methodology, supervision, and writing—review in charge of the whole trial. Y.S. carried out the simulation and wrote the manuscript. C.Y. performed the data processing and assisted with the theoretical analysis. A.H. assisted with the theoretical analysis. All authors have read and agreed to the published version of the manuscript.

Funding: Supported by National Natural Science Foundation of China (No.52075032) and Science and Technology Research and Development Program of China State Railway Group Co., Ltd. (No. K2022J003), and Open and Cooperative Fund of the High Speed Wheel-Rail System Laboratory of NELHSR (2021YJ269).

Institutional Review Board Statement: Not applicable.

Informed Consent Statement: Informed consent was obtained from all subjects involved in the study.

Data Availability Statement: Not applicable.

Conflicts of Interest: The authors declare no conflict of interest.

Nomenclature

Notation	Description
σ_{jk}	Second-order tensor in the global coordinate system
$\sigma_{j'k'}$	Second-order tensor in the local coordinate system
$\alpha_{j'j}, \alpha_{k'k}$	Cosine of the included angle of the corresponding axes of two coordinate systems
$\sigma_1, \sigma_2, \sigma_3$	Principal stress
a_{\perp}	Utilization degree under normal stress in the x-direction of local coordinates
a_{\parallel}	Utilization degree under normal stress in the y-direction of local coordinates
a_{τ}	Utilization degree under shear stress
$[\sigma_{\perp}], [\sigma_{\parallel}], [\tau]$	Allowable fatigue strength values
f_v	Phase effect of σ_{\perp} and σ_{\parallel} ranging from -1.0 to $+1.0$
α_v	Comprehensive degree of utilization
M_{σ}	Moderate stress sensitivity coefficients of normal stress
M_{τ}	Moderate stress sensitivity coefficients of shear stress
N_i	Accumulative cycle number of the measured stress range within the stress range of $\Delta\sigma_i$
$\Delta\sigma_i$	Stress range of the principal stress
$\Delta\sigma_c$	Corresponding fatigue strength at specified cycles; the value depends on different structural classifications
$\Delta\sigma$	Allowable stress range
m_1, m_2	Curve slope of the S-N curve
γ_{Ff}	Partial coefficient of the uncertainty considering the load spectrum and response analysis, generally equal to 1
γ_{mf}	Partial coefficient of the uncertainty considering the material and evaluation uncertainty
σ_m	Mean value of normal stress
σ_a	Normal stress amplitude
σ_{min}	Minimum normal stress
σ_{max}	Maximum normal stress
σ_p	Maximum principal stress
R	Stress ratio of minimum stress-to-maximum stress

References

- Dong, Y.; Teixeira, A.; Soares, C.G. Fatigue reliability analysis of butt welded joints with misalignments based on hotspot stress approach. *Mar. Struct.* **2019**, *65*, 215–228. [[CrossRef](#)]
- Hobbacher, A.F. The IIW fatigue design recommendations-newly revised and expanded. *Weld. World J. Int. Inst. Weld.* **2007**, *51* (Suppl. 1), 243–254.
- Wang, W.J.; Bai, J.; Liu, W. Fatigue assessment of weld structure based on the hot spot stress method. *J. Beijing Jiaotong Univ.* **2017**, *41*, 82–87. (In Chinese)
- Wang, B.J.; Li, Q.; Liu, Z. Research on the Stress Fatigue Assessment about the Hot Spot Stress on the Bogie Frame. *Adv. Mater. Res.* **2011**, *1442*, 328–330. (In Chinese)
- Zhou, Z.Y.; Li, F. Study on Fatigue Analysis of Welded Toes of Plate Structures Using Hot Spot Stress Method Based on Surface Extrapolation. *J. China Railw. Soc.* **2009**, *31*, 90–96. (In Chinese)

6. Mei, J.; Dong, P.; Xing, S.; Vasu, A.; Ganamet, A.; Chung, J.; Mehta, Y. An overview and comparative assessment of approaches to multi-axial fatigue of welded components in codes and standards. *Int. J. Fatigue* **2021**, *146*, 106144. [[CrossRef](#)]
7. Park, W.; Miki, C. Fatigue assessment of large-size welded joints based on the effective notch stress approach. *Int. J. Fatigue* **2008**, *30*, 1556–1568. [[CrossRef](#)]
8. Shen, W.; Yan, R.; Barltrop, N.; Liu, E.; Song, L. A method of determining structural stress for fatigue strength evaluation of welded joints based on notch stress strength theory. *Int. J. Fatigue* **2016**, *90*, 87–98. [[CrossRef](#)]
9. Xu, L.; Kai-Lin, Z.; Yuan, Y.; Xiao-Peng, W. The multi-axle fatigue analysis of welded joints based on notch stress method. *J. Chongqing Univ.* **2017**, *40*, 9–17. (In Chinese)
10. Liu, X.; Zhou, C.; Zhang, K.; Yao, Y. Fatigue Performance Analysis of Bogie Welded Joints Based on Notch Stress Method. *J. China Railw. Soc.* **2017**, *39*, 42–48. (In Chinese)
11. Meneghetti, G.; Campagnolo, A.; Rigon, D. Multiaxial fatigue strength assessment of welded joints using the Peak Stress Method—Part II: Application to structural steel joints. *Int. J. Fatigue* **2017**, *101 Pt 2*, 343–362. [[CrossRef](#)]
12. Xie, S.M.; Zhou, X.K.; Li, X.W.; Li, X.F. Fatigue life prediction for weld line in heavy freight car body based on ASME standard. *Chin. J. Comput. Mech.* **2012**, *29*, 129–134. (In Chinese)
13. Łagoda, T.; Głowacka, K. Fatigue life prediction of welded joints from nominal system to fracture mechanics. *Int. J. Fatigue* **2020**, *137*, 105647. [[CrossRef](#)]
14. Michele, Z.; Vittorio, B.; Giovanni, M. Definition of nominal stress-based FAT classes of complex welded steel structures using the Peak Stress Method. *Procedia Struct. Integr.* **2019**, *19*, 627–636.
15. Susmel, L. Nominal stresses to assess damage in notched additively manufactured steel subjected to constant and variable amplitude multiaxial fatigue loading. *Procedia Struct. Integr.* **2021**, *34*, 178–183. [[CrossRef](#)]
16. Hu, Y.; Wu, S.; Withers, P.J.; Cao, H.; Chen, P.; Zhang, Y.; Shen, Z.; Vojtek, T.; Hutař, P. Corrosion fatigue lifetime assessment of high-speed railway axle EA4T steel with artificial scratch. *Eng. Fract. Mech.* **2021**, *245*, 107588. [[CrossRef](#)]
17. Bokesjö, M.; Al-Emrani, M.; Svensson, T. Fatigue strength of fillet welds subjected to multi-axial stresses. *Int. J. Fatigue* **2012**, *44*, 21–31. [[CrossRef](#)]
18. Zhou, Y.; Tao, J. Theoretical and numerical investigation of stress mode shapes in multi-axial random fatigue. *Mech. Syst. Signal Process.* **2019**, *127*, 499–512. [[CrossRef](#)]
19. Zhang, P.P.; Liu, J.C.; Zhang, B. Assessment Method for Fatigue Strength of EMU Wheel Based on Principal Stress Method and Amendatory Crossland Method. *China Railw. Sci.* **2014**, *35*, 52–57. (In Chinese)
20. An, Q.; Zhao, H.; Liu, Y.A.; Fu, M.H. Fatigue Life Analysis Method for Freight Carbody Based on Multi-axial Criteria. *J. Mech. Eng.* **2019**, *55*, 64–72. [[CrossRef](#)]
21. Wang, L.X. Strength Simulation and Fatigue Life Evaluation of Subway Aluminum Alloy Car Body. Master's Thesis, Dalian Jiao-tong University, Dalian, China, 2020.
22. DVS 1608-2011; Design and Strength Evaluation of Aluminium Alloy Welded Structures in Railway Vehicle Manufacturing. Deutsches Institut für Normung: Berlin, Germany, 2011; 38.
23. BS EN 1999-1-3-2007; Eurocode 9 Design of Aluminium Structures—Part 1–3 Structures Susceptible to Fatigue. The European Union: London, UK, 2007.
24. EN 12663-1:2010; Railway Applications-Structural Requirements of Railway Vehicle Bodies. The European Union: London, UK, 2010.

Disclaimer/Publisher's Note: The statements, opinions and data contained in all publications are solely those of the individual author(s) and contributor(s) and not of MDPI and/or the editor(s). MDPI and/or the editor(s) disclaim responsibility for any injury to people or property resulting from any ideas, methods, instructions or products referred to in the content.